Automatic Intima Media Thickness Detection from the Ultrasound Sequence from the Carotid Artery

Authors
Prof.Nagendra Kumar.M
Associate Professor,Dept of
E&C,SJCIT,Chickballapur,India

MD.Rasheed
Dept of E&C,SJCIT,Chickballapur,India

Jamrud Khan
Asst. Professor, Dept of ECE

Abstract—: Early diagnosis of cardiovascular diseases (CVD) is of utmost importance, since it is one of the largest causes of death in western countries. Fat or cholesterol deposition on the walls of the arteries results in the growth of intima media thickness (IMT). These depositions also called, as carotid plaques are the potential indicators of the CVDs like astherosclerosis. A fully automatic segmentation measurement and tracking algorithm is dealt in this project to extract the intima media complex (IMC) in B mode ultrasound video sequence. The algorithm deals with a two stage procedure in which the first frame of the ultrasound video sequence is segmented out by model based approach. A robust algorithm is used to detect the IMC from the subsequent frames. Adaptive normalized correlation algorithm is used for the first step which prevents false detection of arterial interfaces. The inconsistency in the appearances of the IMC over the cardiac cycles is eliminated in this method. This method would provide accurate detection of the IMC.

INTRODUCTION:

The Carotid Plaque in the human cardiovascular system reflects the ageing problems occurring in the valves. The physical stress occurring on the carotid artery would heavily damage it. The stress is due to the blood pressure, blood flow and tethering due to nearby tissues. The physical estimation like the artery wall structure, thickness, and stiffness are indicators of the presence of carotid plaque in the arteries. High resolution ultrasound imaging has given a more defined visualisation of the carotid artery images. The techniques for the carotid plaque estimation includes measurement of intima media thickness (IMT), severity of stenosis etc,. For decades, the prediction of the carotid plaque was a challenge for medical fraternity in terms of early detection and diagnosis. Different methods as discussed by Efthyvoulos1 has given us the review on different carotid plaque prediction methods. The snake based approach as explained byD. Cheng2and the contouring approach in N. Santhiyakumari3 were used to segment out the IMT. For more accuracy the snake method was introduced with the manual initialisation as referred by C. P. Loizou4. The snake method has a disadvantage , if it is not initialised properly with the region of interest then it would predict a false contour and also a false IMT. So in order to overcome this, morphological methods like the multilevel decomposition were used where the threshold values will be separated as low medium and high values. The more stable plaque values are found in the higher values of the sub bands of the multilevel decomposition as inferred by E. Kyriacou5. In the same line, many different classification techniques are used for the prediction process like, neural classifiers, which include Self Organising Map (SOM) as defined by C. I. Christodoulou6, Back Propagation Network (BPN) as used by S.G.Mougiakakou7, Radial Basis Function (RBF)and Probabilistic Neural Network (PNN) as used by E. Kyriacou5,8. A experiment which included around 32 features containing some gray scale features along with the severity of stenosis were used by Rajendra Acharya.U9 , to classify the symptotic and asymptotic images of carotid artery using the SVM classifier . Güler,N.F10 had employed a procedure through which the Doppler signals from the carotid arteries are gathered as the feature to be trained on the neural network for the carotid plaque prediction. Wismüller, A11 employed SOM in ANN for predicting the segmented carotid plaque on the carotid artery images.NikolaosN12 had defined a method that takes the mean and the standard deviation from the details obtained from different transformation techniques like Discrete wavelet transform, Stationery Wavelet Transform, Wavelet packet and Gabor Transform are trained and tested using SVM and ANN and a comparative study is elaborated. The experiment done by U RajendraAcharya13used three sets of features like ,Discrete wavelet transform that too the horizontal component of it, Higher Order Spectra(HOS) and the texture features like the standard deviation, the third moment of co occurrence matrix and Run Length Non uniformity and the classification technique used was the SVM technique. Radial Basis Function (RBF) was used as the kernel in the classification. Rajendra Acharya14 had introduced the index called Symptomatic Asymptomatic Carotid Index which is a feature generated by the combination of HOS feature, Wavelet feature and the texture feature.

PROPOSED SEGMENTATION ALGORITHM

The developed CAD system relies on a suite of image processing algorithms that embeds a statistical model to

identify the two interfaces that form the IMT complex without any user intervention. The proposed imaging segmentation scheme is based on a spatially continuous vascular model and consists of several steps that will be detailed in the following sub-sections of this paper. An out line of the proposed technique is illustrated in Fig. 2.

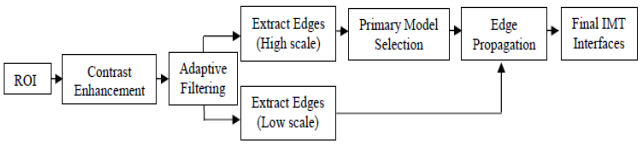

Fig. 2 Schematic representation of the proposed IMT segmentation algorithm.

A. Global Contrast Enhancement

The low contrast between the anatomical structures is one of the main drawbacks associated with the ultrasound imaging modality. Due to low echo responses caused by the ultrasound acquisition process, certain sections of the IMT have a reduced contrast and are not easily distinguishable . In order to improve the appearance of the IMT and facilitate its detection, a global contrast enhancement based on data stretching between two pre-defined thresholds *cmin* and *cmax*, was applied:

$$I_{ce}(x,y)=\frac{255[I(x,y)-c_{\min}]}{c_{\max}-c_{\min}}$$

where $I(x,y)$ is the intensity value of the pixel situated at position (x,y) in the image matrix and $Ice(x,y)$ is the contrast enhanced intensity value. Based on experimentation the values of *cmin* and *cmax* are set to 6 and 150 respectively and are kept constant for all images analyzed in this study. We would also like to note that the selection of these two thresholds proved to be robust irrespective of the ultrasound equipment that has been employed to capture the image data.

B. Automatic Detection of the Region of Interest (ROI)

The ROI where the search for the IMT will be carried out is the area situated above and below the interface that separates the blood and the tissue of the vessel's far wall. To avoid any human intervention, we propose to automatically detect the blood tissue interface (referred to as the Tracked Interface-TI). In order to detect the TI and robustly segment the two image classes (blood and tissue), an adaptive thresholding algorithm [7] followed by an image refinement procedure was applied.

$$h_i=\frac{n_i}{N},\ i\in[0,255],h_i\geq 0,\sum_{i=0}^{255}h_i=1 \qquad (2)$$

In equation (2), *ni* is the number of pixels with grey-level *i*, *N* is the total number of pixels in the image, *N* = *n0+n1+...+n255* and *hi* represents the probability that the pixel with coordinates (x,y) in the contrast enhanced image takes the value *i*. The threshold *k* is automatically detected to maximize the between class variance as follows,

$$\max_{k\in[0,255]}\sigma_B^2(k)=\max\Big\{\sum_{i=0}^{k-1}h_i\Big[\sum_{i=0}^{k-1}(ih_i)/\sum_{i=0}^{k-1}h_i-\sum_{i=0}^{255}(ih_i)\Big]^2+\sum_{i=k}^{255}h_i\Big[\sum_{i=k}^{255}(ih_i)/\sum_{i=k}^{255}h_i-\sum_{i=0}^{255}(ih_i)\Big]^2\Big\} \qquad (3)$$

$$\text{if } I_{ce}(x,y)\leq k \text{ than } I_{ce}(x,y)=0$$
$$\text{if } I_{ce}(x,y)>k \text{ than } I_{ce}(x,y)=255 \qquad (4)$$

The refinement procedure is applied to the image resulting from the thresholding process with the purpose of eliminating the small and spurious regions and obtain a more compact image segmentation. The post processing process is carried out as follows: for each pixel in the thresholded image a histogram $h\Gamma(x,y)$ is constructed in a Γ neighborhood (the value of the mask was chosen so that to be large enough to avoid erroneous assignments):

$$h^{\Gamma}(x,y)=\bigcup_{i=1}^{2}m_i=\{m_1,m_2\} \qquad (5)$$

$$m_1=\int_{\Gamma}\delta(I_{ce}(x,y),255)d\Gamma,\ m_2=\int_{\Gamma}\delta(I_{ce}(x,y),0)d\Gamma$$

$$\delta(i,j)=\begin{cases}1 & i=j\\ 0 & i\neq j\end{cases}$$

In equation (5), Γ is the 7×7 neighborhood around the pixel with coordinates (x,y), *m1* defines the number of white pixels in the mask, while *m2* represents the number of black pixels. If *m1>> m2* then the pixel under analysis belongs to the vessel tissue and it will be assigned a light grey level value, otherwise it corresponds to blood and it be set to 0. In order to facilitate the detection of the TI segment, the borders between the two classes are marked with a white line. The TI interface is generated by the border pixels that simultaneously satisfy the following conditions:

1. $Ice(x,y)=255$;
2. $Ice(x, y+\alpha)=0$;
3. $Ice(x, y-\alpha)>0$.

These conditions evaluate the local distribution of the post processed data around each border pixel ($Ice(x,y)=255$), and they state that the border pixel belongs to the TI interface if it has black neighbours for α pixels above it and bright neighbours for neighbours for α pixels bellow it. (The parameter α is adaptively detected and in this study the search is carried out in the interval [0, 10]). The resulting border segments that satisfy simultaneously the three conditions stated above will be filtered out and only a reduced number of segments will be retained for further analysis. Based on the anatomical structures that compose a carotid ultrasound image, the TI is always the longest continuous segment in the image area that obeys the three conditions discussed above. it is shown the tracked interface for the ultrasound image displayed. Once the TI is identified, the ROI is set using the minimum (*min_y*) and

maximum (*max_y*) coordinates of the tracked interface on the *y*-axis and the width of the original image. To this end, the ROI height is calculated as follows,

$$ROI\_height = (\max\_y - \min\_y) + 2 * smax \quad (6)$$

In equation (6), *smax* is a parameter that sets the model variation above *max_y* and below *min_y* to allow the inclusion of additional information in the ROI that will be necessary in the process of IMT reconstruction. Experiments demonstrated that a *smax* value of 15 is sufficiently large to generate a ROI that covers a large part of the lumen of the carotid artery beyond the adventitia irrespective of the resolution of the ultrasound images. The contrast enhanced image data sampled by the ROI will be further processed for the IMT identification.

C. ROI Pre-Filtering

The purpose of the pre-filtering step is to attenuate the speckle noise in a pre-defined neighborhood calculated around each pixel in the image. The Vector Median Filtering (VMF) [8] is a noise removal scheme that is able to locally adapt to the image content while preserving the contextual image information (edges). To filter the ROI, we iterate through the image with a square mask of size $w \times w$ centered at every pixel in the ROI. Using VMF, every pixel under analysis will be replaced with the pixel from its neighborhood $w \times w$ that returns the minimum Euclidian distance to all other pixels in the neighborhood as follows,

$$I_{ROI}(p_{\min}, q_{\min}) = \left| \min_{(p,q)\in w\times w} \sum_{(u,v)\in w\times w} \left\| I_{ROI}(u,v) - I_{ROI}(p,q) \right\| \right. \quad (7)$$

$$I_{ROI}(x,y) \leftarrow I_{ROI}(p_{\min}, q_{\min})$$

In equation (7), (*pmin*, *qmin*) are the coordinates of the pixel that returns the minimum distance to all pixels located within the mask $w \times w$. To attain feature preservation, the VMF should be applied in a small neighborhood to prevent the edge attenuation that occurs when the VMF filtering scheme is applied for large neighborhoods. In our implementation the neighborhood $w \times w$ is set to 3×3.

D. Initial Edge-Structure Extraction

The next step of the algorithm extracts the initial edge structure of the plausible IMT segments around the area of interest using the Canny edge detector [9]. The reason for selecting Canny for edge detection is that it achieves good detection, good localization and also satisfies the one response criterion by minimizing multiple responses for a single edge. The Canny edge detector extracts the gradient of the image data that is first convolved with a 2D Gaussian filter $G, \nabla[I\ ROI\ (x, y)\quad G(x, y, \square\square)]$, to reduce the occurrence of spurious edges caused by image noise. The scale σ is an essential parameter that sets the size of the Gaussian filter and its value is set in conjunction with the desired level of edge detail: fine versus coarse edges. Taking into consideration that fine edges are numerous and have an irregular (curly) appearance, this generates a difficult scenario when the edge segments are analyzed in the process of IMT detection. To address this issue, the algorithm proposed in this paper adopts a coarse to fine strategy for IMT detection. The initial (coarse) edge detection is performed when the scale of the Gaussian operator is set to σ=1.5. To improve the edge connectivity and remove the weak edges, non-maxima suppression and thresholding with hysteresis are applied [9]. This value of the scale parameter ensures that the irrelevant edges derived from image noise and weak textures are removed and only strong edge features are evaluated to extract the primary IMT model.

I. ONE-DIMENSIONAL FORMULATION

To facilitate the analysis we first consider one-dimensional edge profiles. That is, we will assume that two dimensional edges locally have a constant cross-section in some direction. This would be true for example, of smooth edge contours or of ridges, but not true of corners. We will assume that the image consists of the edge and additive white Gaussian noise. The detection problem is formulated as follows: We begin with an edge of known cross-section bathed in white Gaussian noise as in which shows a step edge. We convolve this with a filter whose impulse response could be illustrated by either. The outputs of the convolutions are shown, respectively. We will mark the center of an edge at a local maximum in the output of the convolution. The design problem then becomes one of finding the filter which gives the best performance with respect to the criteria given below. For example, the filter in performs much better than on this example, because the response of the latter exhibits several local maxima in the region of the edge. In summary, the three performance criteria are as follows:

1) Good detection. There should be a low probability of failing to mark real edge points, and low probability of falsely marking non edge points. Since both these probabilities are monotonically decreasing functions of the output signal-to-noise ratio, this criterion corresponds to maximizing signal-to-noise ratio.

2) Good localization. The points marked as edge points by the operator should be as close as possible to the center of the true edge.

3) Only one response to a single edge. This is implicitly captured in the first criterion since when there are two responses to the same edge, one of them must be considered false. However, the mathematical form of the first criterion did not capture the multiple response requirement and it had to be made explicit.

II. Detection and Localization Criteria

A crucial step in our method is to capture the intuitive criteria given above in a mathematical form which is readily solvable. We deal first with signal-to-noise ratio and localization. Let the impulse response of the filter be f(x),and denote the edge itself by G(x). We will assume that the edge is centered at x = 0. Then the response of the filter to this edge at its center HG is given by a convolution integral:

$$H_G = \int_{-W}^{+W} G(-x)\, f(x)\, dx \qquad (1)$$

III. Eliminating Multiple Responses

In our specification of the edge detection problem, we decided that edges would be marked at local maxima in the response of a linear filter applied to the image. The detection criterion given in the last section measures the effectiveness of the filter in discriminating between signal and noise at the center of an edge. It does not take into account the behavior of the filter nearby the edge center. The first two criteria can be trivially maximized as fol-lows. From the Schwarz inequality for integrals we can show that SNR (3) is bounded above by

$$n_0^{-1} \sqrt{\int_{-W}^{+W} G^2(x)\, dx}$$

and localization (9) by

$$n_0^{-1} \sqrt{\int_{-W}^{+W} G'^2(x)\, dx}.$$

Methodology:

Stereo matching aims to obtain 3D information by finding the correct correspondence between images captured from different point of views or at different times. However, finding the accurate correspondence is not an easy task; there exist a number of difficulties, such as occluded regions, texture less regions, and object boundaries. This issue has been an important area of research in the past several decades, and considerable progress has been made with respect to the problem surrounding stereo matching algorithms. These algorithms are based on a common assumption that corresponding pixels have similar color values, an assumption we refer to as color consistency. As a consequence, a majority of these utilize a data cost which includes simple L1 or L2 difference of intensities or color values of corresponding pixels. However, it should be noted that these methods do not hold good for stereo images which do not have similar corresponding color values. Nonetheless, a few studies have been performed in order to solve this problem. In a real scenario, various factors prevent two corresponding pixels from having the same color value. One major preventing factor is a radiometric change, which includes lighting geometry, illuminant color, and camera device changes between stereo images. In this paper, we present a new stereo matching measure that is robust in handling various radiometric changes, including local radiometric variations caused by varying lighting geometry, as well as global radiometric variations that are brought about by changes in illuminant color and camera parameter . It should be noted that this paper is based on the assumption of the Lambertian world. Under the assumption, the color formation process was explicitly modeled, unlike other methods. Then, we have extracted the invariant color information from the color model and thereby propose, in this paper, a new matching measure, called Adaptive Normalized Cross Correlation (ANCC), which is robust to various radiometric changes.

Experimental Results:

The numerical results indicate that no significant differences between the ground truth IMT and the segmented IMT occur, and we can conclude that the proposed approach is able to accurately detect the IMT. the primary IMT model that represents an accurate marker that allows the identification of the IMT segments in the edge data extracted at a low scale. The low scale edge structure is shown in Fig. 4d). To obtain good edge estimates, the edge segments are analyzed using the least square fitting principle detailed in Section III.E and the result is shown in Fig. 4e). The next step of the algorithm propagates the information associated with the primary model to select the lower scale edge segments that are spatially contiguous and consistent with the geometrical characteristics associated with the primary IMT model. To achieve this, a list of edge terminators for each segment of the primary model is extracted. Then, for each edge terminator we search for edge pixels in the low scale edge data and the reconstruction process is initiated in an iterative fashion until the last segment that obeys the primary model geometric conditions is reached. This process is applied for all edge terminators and the reconstructed structure is added to the primary model. The final IMT segmentation for the image in is shown in Fig. 4f).

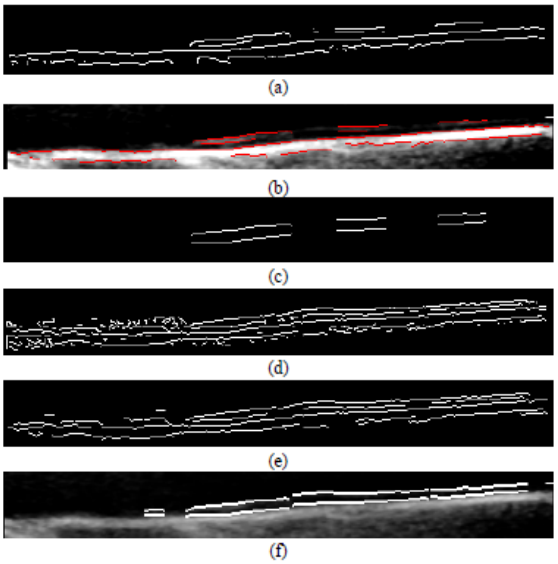

Fig. 4. Intermediate steps of the proposed segmentation algorithm. (a) Initial edge structure. (b) The filtered edges that are quasi-parallel to the TI are superimposed on the contrast-enhanced image. (c) The primary IMT model. (d) The lower scale edges. (e) Lower scale edges filtered using least square fitting. (f) The final pair of lines of the IMT complex resulting after the edge data reconstruction (the maximum IMT value calculated by our algorithm is 0.70 mm).

CONCLUSION:

The major aim of this paper was to introduce a novel algorithm for the segmentation of the IMT in longitudinal carotid ultrasound images. The main novelty of this approach resides in the development of an unsupervised algorithm that embeds a statistical IMT model in a coarse to fine fashion. The proposed algorithm proved to produce accurate segmentation results when applied to various carotid ultrasound images that are characterized by low resolution and high level of image noise. This research is ongoing and we plan to extend the capabilities of the proposed CAD system to automatically measure the IMT in multidimensional (2D+time) ultrasound carotid data in order to allow the calculation of dynamical properties of the carotid artery. Future additional testing of the algorithm will also include images from patients with more advanced disease, i.e. with focal thickenings and actual plaques.

REFERENCES:

[1] Efthyvoulos C. Kyriacou, Member, IEEE, Constantinos Pattichis, Senior Member, IEEE, Marios Pattichis, Senior Member , IEEE, Christos Loizou, Member , IEEE, Christodoulos Christodoulou, Stavros K. Kakkos, and Andrew Nicolaides"A Review of Noninvasive Ultrasound Image Processing Methods in the Analysis of Carotid Plaque Morphology for the Assessment of Stroke Risk"

[2]D. Cheng, A. Schmidt Trucksaess, K. Cheng, and H. Burkhardt, "Using snakes to detect the intimal and adventitial layers of the common carotid artery wall in sonographic images," Comput. Methods Program. Biol., vol. 67, no. 1, pp. 27–37, 2002.

[3] N. Santhiya kumari and M. Madheswaran, "Extraction of intima media layer of arteriacarotis and evaluation of its thickness using active contour approach," in Proc. Int. Conf. Intell. Adv. Syst., 25–28 Nov. 2007, pp. 582–586

[4] C. P. Loizou, C. S. Pattichis, M. Pantziaris, T. Tyllis, and A. Nicolaides, "Snakes based segmentation of the common carotid artery intima media," Med. Biol. Eng. Comput., vol. 45, no. 1, pp. 35–49, 2007.

[5] E. Kyriacou, M. Pattichis, C. S. Pattichis, A. Mavrommatis, C. I. Christodoulou, S. Kakkos, and A. Nicolaides, "Classification of atherosclerotic carotid plaques using morphological analysis on ultrasound images," J. Appl. Intell., vol. 30, no. 1, pp. 3–23, 2009.

[6] C. I. Christodoulou, C. S. Pattichis, M. Pantziaris, and A. Nicolaides, "Texture based classification of atherosclerotic carotid plaques," IEEE Trans. Med. Imag., vol. 22, no. 7, pp. 902–912, Jul. 2003.

[7] S.G.Mougiakakou,S.Golemati,I.Gousias,A.Nicolaides,andK.Nikita, "Computeraided diagnosis of carotid atherosclerosis based on ultrasound image statistics, laws' texture and neural networks," Ultrasound Med. Biol., vol. 33, no. 1, pp. 26–36, 2007.

[8] E. C. Kyriacou, C. S. Pattichis, M. A. Karaolis, C. P. Loizou, C. T. Christodoulou, M. S. Pattichis, S. Kakkos, and A. Nicolaides "An medicine and biology magazine," Special Issue on Image, Signal and Distributed Data Processing for Networked Health Applications, vol. 26, no. 5, pp. 43–50, Sep./Oct. 2007.

[9] RajendraAcharya U., Muthu Rama Krishnan M., VinithaSree S. ,Sanches J., Shafique S., Nicolaides A., Pedro L.M., Suri, J.S. Plaque Tissue Characterization and Classification in Ultrasound Carotid Scans: A Paradigm for Vascular Feature Amalgamation ,IEEE Trans.Intrumentation and measurement, Volume:62 , Issue: 2 392 – 400 , Feb. 2013

[10] Güler,N.F.,andU¨beyli,E.D.,Waveletbasedneuralnetworkanalysis of ophthalmic artery Doppler signals. Comput. Biol. Med. 34(7):601–613, 2004.

[11].Wismüller, A., Vietze, F., Behrends, J., MeyerBaese, A., Reiser, M., Ritter, H.: Fully Automated Biomedical Image Segmentation by SelfOrganized Model Adaptation.Neural Networks, 17 (2004), 1327–1344

[12] Nikolaos N. Tsiaparas, SpyrettaGolemati, Member, IEEE, IoannisAndreadis, John S. Stoitsis, Member, IEEE, IoannisValavanis, Member, IEEE, and Konstantina S. Nikita, Senior Member, IEEE, Comparison of Multiresolution Features for Texture Classification of Carotid Atherosclerosis From B Mode Ultrasound IEEE TRANSACTIONS ON INFORMATION TECHNOLOGY IN BIOMEDICINE, VOL. 15, NO. 1, JANUARY 2011

[13] U Rajendra Acharya, Oliver Faust, VinithaSree S., AngPengChuan Alvin, GanapathyKrishnamurthi, Jos´e C. R. Seabra, JoãoSanches, Jasjit S Suri,AtheromaticTM: Symptomatic vs. Asymptomatic Classification O f Carotid Ultrasound Plaque using a combination of HOS, DWT & Texture EMBS Boston Conference 2011

[14] U. RajendraAcharya, Oliver Faust, VinithaSree S., A.P.C. Alvin, GanapathyKrishnamurthi, José C.R. Seabra, JoãoSanches, Jasjit S. SuriUnderstanding symptomatology of atherosclerotic plaque by imagebased tissue characterization ,Computer Methods and Programs in Biomedicine (2012).